JOURNAL OF MATERIALS SCIENCE 13 (1978) 2627–2636

The compression creep behaviour of silicon nitride ceramics

J. M. BIRCH*, B. WILSHIRE
Department of Metallurgy and Materials Technology, University College, Singleton Park, Swansea, UK

A comparison has been made of the compression creep characteristics of samples of reaction-bonded and hot-pressed silicon nitride, a sialon and silicon carbide. In addition, the effects of factors such as oxide additions and fabrication variables on the creep resistance of reaction-bonded material and the influence of dispersions of SiC particles on the creep properties of hot-pressed silicon nitride have been considered. For the entire range of materials examined, the creep behaviour appears to be determined primarily by the rate at which the development of grain boundary microcracks allows relative movement of the crystals to take place.

1. Introduction

Interest in high-performance gas turbines for transportation [1] and power generation [2, 3] has led to increasing attention being devoted to the development and study of silicon nitride ceramics. Intricate components can be fabricated by producing silicon powder compacts of the shape required, then nitriding at ~1650 K. The reaction-bonded silicon nitride (RBSN) obtained by this procedure is a product of mixed α- and β-silicon nitride having ~25% porosity. In addition, less complex shapes in predominantly β-silicon nitride can be prepared in a fully dense form by hot-pressing nitrided silicon powder with a suitable additive (giving hot-pressed silicon nitride, HPSN). More recently, a new range of materials has been developed, based on phases in the silicon–aluminium–oxygen–nitrogen and related systems, which are usually referred to as sialons [4].

In view of the potential importance of silicon nitride ceramics for high-temperature applications, a number of investigations have been aimed at determining the creep behaviour of these materials [5–13]. However, comparisons of creep properties have been hindered by differences in the type and precision of the testing procedures employed in these studies. In the present work, the compression creep characteristics of a selected range of silicon nitride ceramics has been examined, using high-precision, constant stress equipment [14]. Compression testing has the advantage that only small quantities of material are needed to evaluate the creep properties, e.g. in this case, the cylindrical testpieces used were 6.4 mm long and 3.18 mm diameter. Subsequent programmes were then undertaken to consider:

(a) the extent to which variations in fabrication procedure can affect the creep behaviour of reaction-bonded silicon nitride;

(b) the influence of dispersions of silicon carbide particles on the creep strength of hot-pressed silicon nitride.

2. Creep behaviour of silicon nitride ceramics

As there is a wide range of silicon nitride materials available, the present investigation was restricted to a selected number of typical products. The RBSN, supplied by the Admiralty Materials Laboratory, was produced from Dunstan and Wragg silicon powder of ~25 μm average particle size. Bars of compacted silicon powder showed weight gains of ~63% during nitriding, with room temperature bend strengths in the range 227 to 248 $MN\,m^{-2}$ and densities of ~2.6 $Mg\,m^{-3}$. The structure and properties of reaction-bonded materials have been discussed previously [15].

*Now with the BNF Metals Technology Centre, Wantage.

The hot-pressed silicon nitride testpieces were ultrasonically trepanned from a tile (No. 247) supplied by J. Lucas Ltd. (referred to as HPSN-1). This form of silicon nitride, containing ~2% MgO, was close to theoretical density (~3.2 Mg m^{-3}) and was composed almost entirely of β-Si_3N_4, with a crystal size of ~1 μm [16]. Since the creep properties of hot-pressed materials appear to be markedly dependent on the impurity levels present [13], a further programme was carried out using samples obtained from the Plessey Co. Ltd. (designated HPSN-2). This material was selected since it had a density and crystal size comparable with the HPSN-1 samples, but had been produced by hot-pressing at 2073 K with ~5% MgO.

The Lucas sialon ($z = 1$) was made by reacting Si_3N_4 with AlN and SiO_2 and contained only minor additions of metal oxides (Tile No. 159). The density was 3.05 Mg m^{-3} and the bend strengths recorded at room temperature and 1473 K were 475 and 462 MN m^{-2} respectively.

2.1. Creep characteristics of silicon nitride ceramics

The compressive creep properties of the various silicon nitride ceramics are presented in Figs. 1 to 3, which also include the results recorded in a limited series of tests carried out for sintered silicon carbide. All of the materials showed normal primary and secondary creep curves (Fig. 1) i.e. the rapid initial creep rates observed immediately after loading were found to decrease continuously until a steady state appeared to be attained. For the RBSN, results obtained under identical creep conditions for a number of different samples nitrided in the same batch showed that the secondary creep rate was reproducible to ±20% [17, 18]. Although most of the tests were discontinued during secondary creep, some tests for both the RBSN and HPSN samples were allowed to proceed showing that the constant creep rate did not continue indefinitely, but eventually accelerated during the tertiary stage, leading to fracture. The occurrence of a tertiary stage indicates that cracks cannot propagate rapidly during compression tests. In contrast, tertiary creep has only rarely been detected under bend or tensile creep conditions with these materials.

In all cases, the dependence of the secondary creep rate, $\dot{\epsilon}_s$, on stress (σ) and temperature (T) could be described by the equation

$$\dot{\epsilon}_s = A\sigma^n \exp(-Q_c/RT) \quad (1)$$

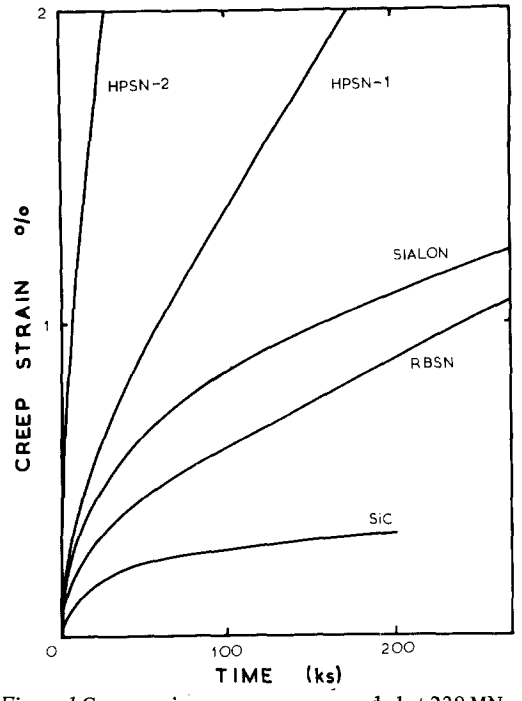

Figure 1 Compression creep curves recorded at 238 MN m^{-2} and 1623 K for samples of reaction-bonded and hot-pressed silicon nitride, a sialon ($z = 1$) and sintered silicon carbide. The hot-pressed sample (designated HPSN-1) contained ~2% MgO compared with ~5% MgO for the material labelled HPSN-2.

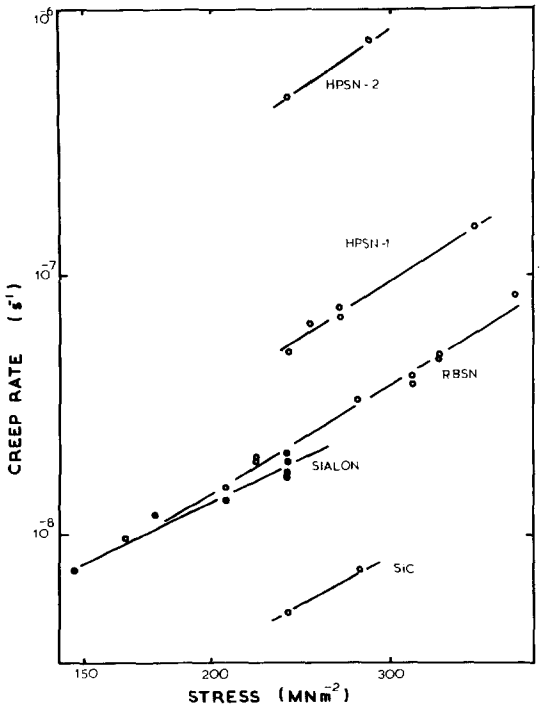

Figure 2 Stress dependence of the secondary creep rate ($\dot{\epsilon}_s$) for samples of reaction-bonded and hot-pressed silicon nitride, a sialon ($z = 1$) and sintered silicon carbide for compression creep tests carried out at 1623 K.

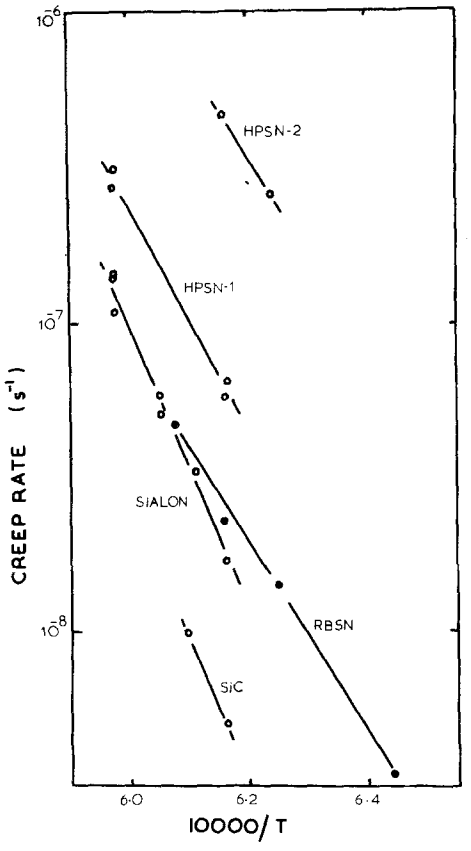

Figure 3 Temperature dependence of the secondary creep rate ($\dot{\epsilon}_s$) for samples of reaction-bonded and hot-pressed silicon nitride, a sialon ($z = 1$) and sintered silicon carbide for compression creep tests carried out at 238 MN m^{-2}.

The stress exponent (n) was 2.1 to 2.4 for the materials studied, indicating that the relative order of creep resistance (Fig. 1) did not alter over the stress range considered (Fig. 2). The activation energy for creep (Q_c) was ~650 kJ mol^{-1} for both the RBSN and HPSN samples, with those for SiC and the sialon sample appearing to be slightly higher at 730 and 850 kJ mol^{-1} respectively (Fig. 3). Values of n and Q_c of this order have been reported by other investigators for creep of RBSN in bend [7, 9, 10] and for HPSN in bend [11] and tension [13]. It has also been found that, for the present reaction bonded material, similar Q_c values were recorded [18] for creep in tension and for stress-rupture experiments.

No specific conclusions can be drawn from the exact differences in the creep resistance of these materials since the high temperature properties of each type of product are known to vary depending on the impurity levels [9, 10, 13, 19, 20] and the detailed fabrication procedures used [9, 10, 21, 22], e.g. the decrease in creep strength associated with the presence of a higher MgO content is evident from the results obtained for the two samples of hot-pressed silicon nitride considered (Figs. 1 to 3). Similarly, the creep strength of sialons has been found to depend not only on the impurity levels but also on the Si/Al ratio [12, 22]. It is noteworthy, however, that the creep behaviour of the sialon sample tested in the present programme was similar to that for the RBSN examined, indicating that sialons can be produced having a creep resistance at least equal to that of reaction-bonded materials (Figs. 1 to 3). In addition, the present results are consistent with the low creep strains and high creep strengths which have been reported for silicon carbide samples [23–26].

2.2. Deformation processes during creep of silicon nitride ceramics

Although dislocations have been observed in silicon nitride samples [11, 13, 27], it is usually considered that plastic strain as a result of slip within the grains can play only a minor role in the deformation of silicon nitride at temperatures below ~2000 K [13]. A similar conclusion can be drawn for silicon carbide [28]. As a result, a number of deformation mechanisms dependent on the presence of grain boundaries have been considered in order to account for the observed creep behaviour. These include diffusional creep processes [29–31], grain boundary sliding controlled by the viscosity of the impurity phases at crystal boundaries [13], dissolution and redeposition of material [22], and transfer of the viscous phases from boundaries under compression to those under tension [32]. Support for the view that viscous flow of impurity phases controls the creep behaviour of RBSN and HPSN [13] has been taken from the fact that the activation energy for flow of certain silicate glasses [33] can be of the order of the observed values for creep (~ 650 kJ mol^{-1}). Furthermore, the results recorded for the hot-pressed materials (Figs. 1 to 3) demonstrate the importance of the impurity phases in determining the creep resistance. However, the form of the creep curves (Fig. 1) and also the stress- and temperature-dependence of the creep rate (Figs. 2 and 3) are similar for all of the products studied. This evidence suggests that, despite marked differences in composition, amount and distribution of impurity phases, the rate de-

termining process is essentially the same for the present range of materials.

For HPSN [13] and RBSN [18], it has been observed that the applied stress required to obtain a given creep rate in compression is about an order of magnitude greater than that needed under tensile creep conditions. Deformation mechanisms dependent on the presence of viscous phases at the grain boundaries would be expected to result in comparable creep rates in tension and compression. It has therefore been suggested [17, 18] that this major difference in the creep strength in tension and compression is a result of the deformation processes being controlled by the fracture characteristics of these materials. For both RBSN [10] and HPSN [11, 13], cracks have been observed to develop at grain boundaries during creep. The formation of grain boundary cavities and cracks depends on the magnitude of the tensile stresses developed across the boundaries. Under compression creep conditions, the maximum tensile stresses developed (across boundaries parallel to the specimen axis) are only about one tenth of the applied compression stress [17]. The ten-fold difference in creep strength in tension and compression can therefore be accounted for on the basis that the microcrack formation necessary to accommodate relative movement of the crystals, rather than the grain boundary sliding itself, is the rate-controlling process with this type of ceramic [17, 18].

This model is consistent with the observation that the activation energies for creep of silicon nitride materials ($Q_c \simeq 650\,kJ\,mol^{-1}$) are similar to the values reported for stress-rupture [18] and crack growth [34–36]. The n values recorded (Fig. 2) are also compatible with the stress exponent (~ 2) which can be derived for grain boundary sliding controlled by crack development [37, 38]. With this approach, differences in crystal size, porosity and impurity levels would modify the creep resistance by influencing the ease of grain boundary sliding and crack formation. In addition, processes such as dissolution/redeposition and viscous phase transfer could contribute independently to the overall creep strain, depending on the creep conditions. The creep resistance of silicon nitride ceramics (reflected in the magnitude of the parameter, A, in Equation 1) would then depend not only on the type of material (Figs. 1 to 3) but also on the extent to which variations in fabrication procedure affect the microstructure of the product.

3. Factors affecting the creep strength of reaction-bonded silicon nitride

Several previous investigations have indicated that the creep strength of reaction-bonded silicon nitride depends upon a number of variables including the impurity levels [9, 10], the α/β ratio [11, 21], the amount and size distribution of pores [7, 21, 39] and the nitriding atmosphere [9]. In addition, the strength can be affected by the test atmosphere, with the creep rates recorded being about 30 times greater in air than in vacuum [40]. However, the effects of variations in test atmosphere appear to be less significant with material of relatively high density ($\sim 2.6\,Mg\,m^{-3}$) when the creep rates in air were found to be only $\sim 20\%$ more rapid than those in argon [17]. In the present programme, a study has been made of the extent to which the creep behaviour of reaction-bonded silicon nitride is influenced by:

(i) variations in the purity and size distribution of the initial silicon powders and the weight gains during nitriding;

(ii) the presence of minor quantities of refractory oxides.

3.1. The effects of silicon powder characteristics

The effects of purity and size distribution of the initial silicon powders were assessed by considering the creep properties of the series of reaction-bonded samples listed in Table I [41]. The compression creep curves obtained in duplicate tests at 1623 K and $145\,MN\,m^{-2}$ for these samples is shown in

TABLE I Fabrication details of reaction-bonded silicon nitride materials

Silicon powder description	Average silicon particle size (μm)	Weight gain (%) during nitriding
(a) Commercial purity (Murex)	12	60
(b) Commercial purity (Murex)	12	63
(c) Commercial purity (Dunstan and Wragg)	25	60
(d) High purity (Hostombe)	15	63
(e) Commercial purity (Dunstan and Wragg)	25	63

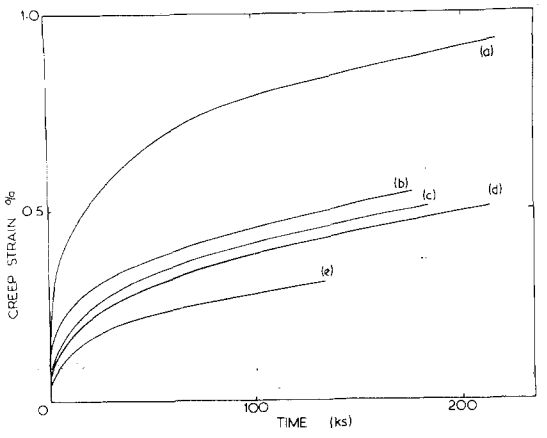

Figure 4 Compression creep curves for samples of reaction-bonded silicon nitride tested at 145 MN m^{-2} and 1623 K. The materials examined are designated (a) 12 μm Si powder (Murex) having weight gain of 60%, (b) 12 μm Si powder (Murex) having weight gain of 63%, (c) 25 μm Si powder (D-W) having weight gain of 60%, (d) 15 μm Si powder (Hostombe) having weight gain of 63%, (e) 25 μm Si powder (D-W) having weight gain of 63%.

Fig. 4. Although all of the materials attained similar secondary creep rates, significant differences were found in the primary creep strains exhibited.

Since the commercial-purity Murex and the high-purity Hostombe powders had comparable initial powder sizes and the samples produced showed similar weight gains during nitriding (~63%), comparison of their creep behaviour allowed the effects of variations in powder purity to be considered. The similarity of the creep curves recorded (Labelled b and d in Fig. 4) suggests that improving the purity of the initial silicon powder beyond normal commercial levels does not significantly alter the creep behaviour of RBSN.

The effects on creep strength of variations in the weight gain during nitriding can be assessed by comparing the results obtained for samples produced from both the Dunstan and Wragg 25 μm powder (i.e. curves c and e in Fig. 4) and the Murex 12 μm powder (i.e. curves a and b), which had been nitrided in different batches. In both cases, the primary creep strains recorded were larger for material of lower weight gain during nitriding.

The present results also provide an indication of the influence of the initial silicon powder size on the creep behaviour. This can be shown by comparing the creep curves recorded for samples produced from the 12 μm Murex powder and the 25 μm Dunstan and Wragg powder. When compacts of these powders were nitrided to give weight gains of either ~60% (i.e. curves a and c respectively) or ~63% (i.e. curves b and e respectively in Fig. 4), it appears that increasing the average silicon powder size results in material exhibiting lower primary creep strains.

Minor differences in fabrication procedure can therefore modify the creep behaviour specified in terms of the time to achieve a given total creep strain. The variables appear to influence the creep properties by affecting the crystal size and pore distribution of the reaction-bonded silicon nitride.

3.2. The effects of oxide impregnation

In order to examine the effects of small quantities of refractory oxides on the creep strength, a series of RBSN samples were prepared which had been impregnated with nitrate solutions and then decomposed at 1023 K [42] Testpieces were

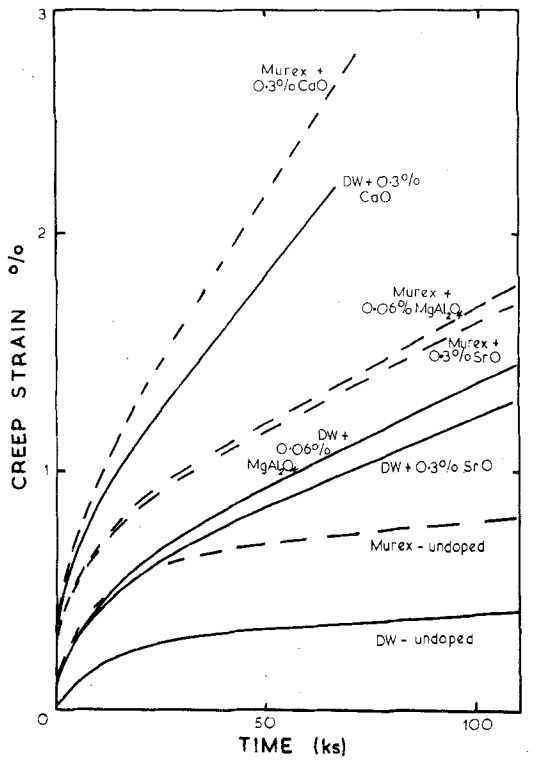

Figure 5 Compression creep curves for reaction-bonded silicon nitride samples tested at 145 MN m^{-2} and 1623 K. The samples were produced from either Murex 12 μm silicon powder (shown as — — —) or Dunstan and Wragg 25 μm silicon powder (shown as ——). Both types of materials were impregnated with 0.3% SrO_2, 0.06% $MgAl_2O_4$ or 0.3% CaO respectively.

produced from materials made using both 12 μm silicon powder (Murex) and 25 μm powder (Dunstan and Wragg), nitrided under the same conditions as those giving weight gains of ~60% (Table I). The impregnated samples, which contained 0.3% CaO, 0.3% SrO and 0.06% $MgAl_2O_4$ respectively, were also tested in compression at 1623 K and 145 MN m^{-2}. The creep curves recorded are presented in Fig. 5. As found for the undoped specimens (Fig. 4), the primary creep strains displayed by the samples produced from the 12 μm Murex powder were consistently larger than those exhibited by the testpieces fabricated using 25 μm Dunstan and Wragg powder (Fig. 5). The effects on the creep behaviour caused by the impregnation with the different oxides were, however, the same for samples made using both types of powder. Adding 0.3% SrO was found to increase the secondary creep rate by a factor of 7 to 10, adding 0.06% $MgAl_2O_4$ increased the rate by 8 to 10 whilst adding 0.3% CaO decreased the creep resistance by 25 to 30 (Fig. 5) The presence of minor quantities of refractory oxides can therefore cause a significant decrease in the creep resistance of reaction-bonded materials. It would appear that these additions affect the amount and compositions of the impurity phases present, increasing the ease of grain boundary sliding and crack development.

4. The effects of silicon carbide additions on the creep behaviour of hot-pressed silicon nitride

Several studies have shown that the creep strength of HPSN can be increased considerably by minimizing the impurity contents, particularly the CaO levels [13, 19, 20]. Another possible method of improving the creep resistance of silicon nitride involves the incorporation of a dispersion of silicon carbide particles [5, 43]. Silicon carbide has generally been found to exhibit a higher creep strength than silicon nitride materials (as illustrated in Figs. 1 to 3) and several early studies suggested that silicon carbide additions result in improved creep resistance [5, 43]. In contrast, some recent work has indicated that the room temperature strength decreases in proportion to the amount of silicon carbide added [41, 44]. A survey was therefore undertaken to consider the effects of silicon carbide additions on the compression creep strength of HPSN.

TABLE II The volume fractions and average particle sizes of the silicon carbide additions made to hot-pressed silicon nitride

Mean silicon carbide powder size (μm)	Vol % SiC						
2	0	5	10	15	20	30	40
3			10				
13	0	5	10	15	20	30	40
53			10				

4.1. Creep behaviour of Si_3N_4/SiC materials

A wide range of samples were produced by mixing silicon nitride and carbide powders before pressing at 2073 K with ~5% MgO, giving materials with densities in the range 3.2 to 3.23 Mg m^{-3}. The volume fractions and the average SiC powder sizes examined are given in Table II. Typical creep curves for compression tests carried out at 1623 K and 238 MN m^{-2} are shown in Fig. 6. Although the creep strength of silicon carbide is markedly greater than that for the HPSN (Figs. 1 to 3), it was established that the presence of a dispersion of SiC particles could detrimentally affect the creep behaviour of the hot-pressed silicon nitride (Fig. 7). Additions of carbide of 2 to 3 μm average particle diameter (which was comparable with the crystal size of the HPSN) did not change the creep rate significantly (Fig. 7) whereas additions of

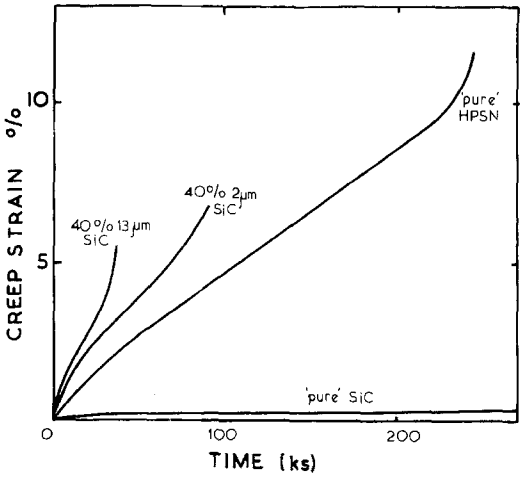

Figure 6 Compression creep curves obtained at 238 MN m^{-2} and 1623 K for hot-pressed silicon nitride and HPSN samples containing a dispersion of silicon carbide particles. The creep curve for sintered silicon carbide under these testing conditions is included for comparison.

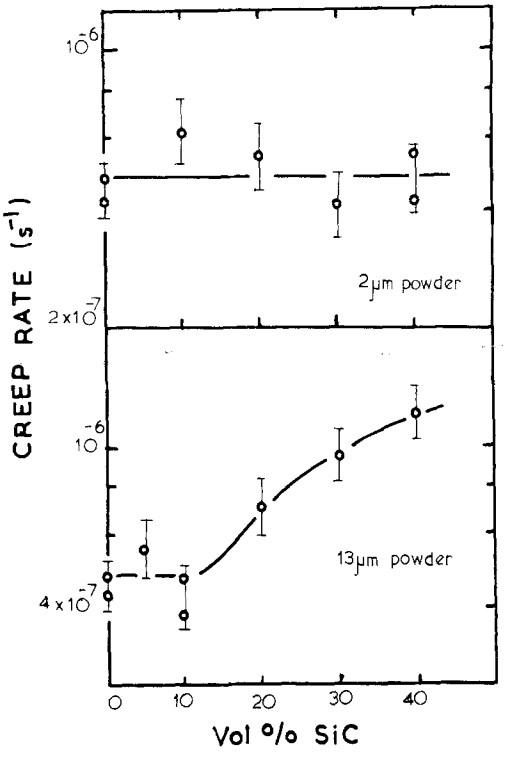

Figure 7 The dependence of the secondary creep rate, $\dot{\epsilon}_s$, of hot-pressed silicon nitride on the volume fraction of silicon carbide additions of 2 μm and 13 μm average diameter for tests carried out at 238 MN m^{-2} and 1623 K.

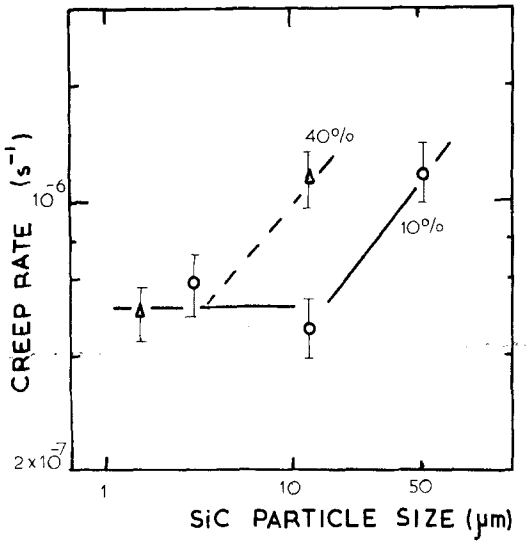

Figure 8 The dependence of the secondary creep rate, $\dot{\epsilon}_s$, of hot-pressed silicon nitride on the average size of the silicon carbide particles for samples containing 10 vol% (○) and 40 vol % SiC (△) for tests carried out at 238 MN m^{-2} and 1623 K.

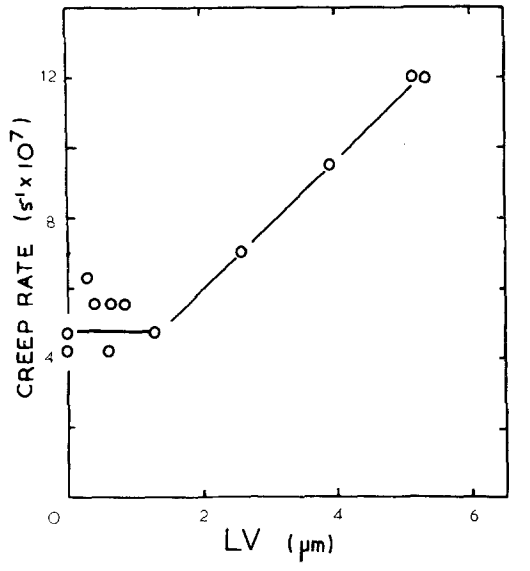

Figure 9 The dependence of the secondary creep rate, $\dot{\epsilon}_s$, on the product of the average size (L) and the volume fraction (V) of the silicon carbide particles.

~13 μm SiC at concentrations above ~15 vol% caused an increase in creep rate. The influence of the ~53 μm particles was even more pronounced.

The effect of variations in the mean particle size of the silicon carbide additions on the secondary creep rates recorded is plotted directly in Fig. 8. It can be seen that the creep strength decreased only when particles above a threshold size were introduced, the threshold size decreasing with increasing volume fraction of carbide. The results for all combinations of mean size and volume fraction can be correlated by plotting the observed secondary creep rate as a function of the product of particle diameter (L) and volume fraction (V). Then, over the range tested, once a threshold value was exceeded the creep rate appears to be linearly dependent on LV (Fig. 9).

Determinations of the stress- and temperature-dependence of creep of the Si_3N_4/SiC materials were carried out by making stress or temperature changes during secondary creep. When the results were expressed as:

$$\dot{\epsilon}_s = A\sigma^n \exp(-Q_c/RT)$$

the stress exponent (n) was ~2 and the activation energy for creep (Q_c) was ~650 kJ mol^{-1} for the entire range of samples examined.

It must be recognized that the effect of the SiC additions on the creep rate was not marked, the maximum increase in creep rate observed being ~3 to 4 (Fig. 9). Yet, the additions had a more significant effect on the creep ductility, the strain to the onset of tertiary creep being only about

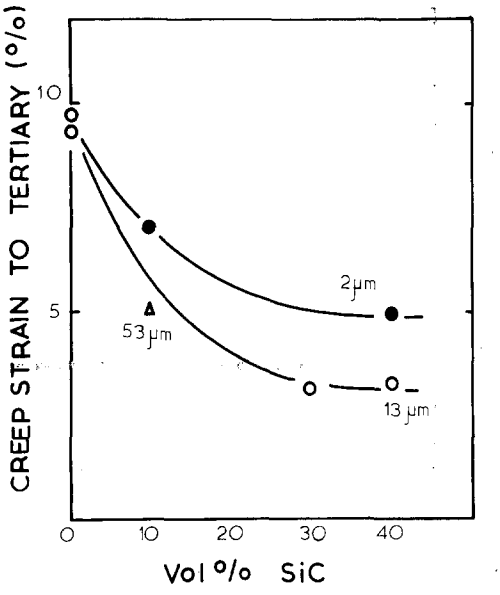

Figure 10 The dependence of the total creep strain to the onset of tertiary creep on the volume fraction of silicon carbide addtions of 2 μm and 13 μm average diameter for tests carried out at 238 MN m^{-2} and 1623 K.

half to one third of the value obtained for HPSN (Fig. 10). The total strain to fracture was found to be lowered to a similar extent.

4.2. The influence of SiC additions on the deformation characteristics of HPSN

The observation that the form of the creep curve and the stress- and temperature-dependence of creep were unaffected by the silicon carbide particles suggests that the mechanism of creep is the same for the range of additions studied. The effects of incorporating the SiC powders can then be considered on the basis that the creep rate is determined primarily by the development of microcracks controlling the relative movement of the crystals [17, 18].

Under compression creep conditions, cracks form preferentially on boundaries parallel to the compression axis, i.e. on boundaries across which a tensile stress is developed. The ease of formation of cracks along the boundaries of the SiC particles is shown in Fig. 11. Silicon carbide particles having a crystal size (~2 to 3 μm) similar to that of the silicon nitride matrix would then be expected to have little influence on the crack development and, hence, on the creep rates observed. However, the incorporation of larger particle sizes would introduce grain boundary facets along which large cracks can develop (Fig. 11) affecting both the

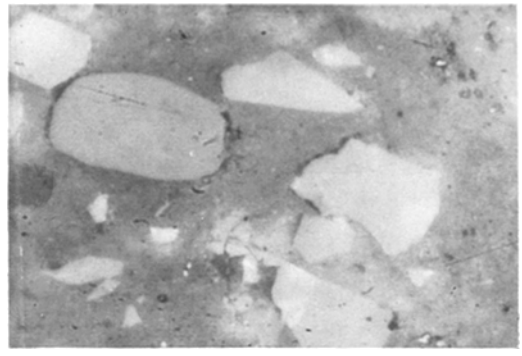

Figure 11 Microstructure of hot-pressed silicon nitride containing 30 vol% of 13 μm silicon carbide particles. After a total creep strain of 0.04 during a test at 238 MN m^{-2} and 1623 K, cavities and cracks can be detected at the boundaries of the carbide particles which are parallel to the compression axis (vertical) (X 660).

creep rate (Figs. 7 to 9) and the creep ductilities (Fig. 10). The dependence of the creep rate on the product LV (Fig. 9) can then be accounted for in terms of this quantity providing a measure of the total grain boundary area of carbide additions.

A further significant feature observed in the present programme was that the presence of a dispersion of large silicon carbide particles introduced an orientation effect. All of the results presented in Figs. 6 to 10 were obtained for compression samples tested with the specimen axis parallel to the pressing direction. However, samples containing 0 and 30% of the 13 μm SiC powder were also prepared with the specimen axis perpendicular to the direction of pressing. The specimens containing the SiC particles gave, on testing perpendicular to the pressing direction, secondary creep rates which were ~ 3 times faster than those recorded for testpieces with the pressing direction parallel to the compression axis. In contrast, the standard HPSN showed no orientation effect. Microstructural examination established that the SiC powder was not perfectly equiaxed, and that the long axis became aligned perpendicular to the pressing direction (Fig. 12). Since cracks form predominantly on boundaries parallel to the compressive stress axis, an explanation can be provided for the orientation effect observed with samples containing the SiC powder. When the specimens were tested with the compression axis perpendicular to the pressing direction, faster creep rates would be expected since the alignment results in a greater effective surface area of carbide particles parallel

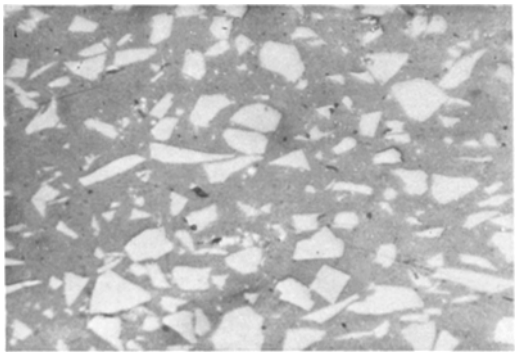

Figure 12 Microstructure of hot-pressed silicon nitride containing 30 vol% of 13 μm silicon carbide particles. The pressing direction is vertical. (× 170).

to the compression axis on which large cracks can develop (Fig. 11).

5. Conclusions

(1) Compression creep tests carried out over a range of stresses at temperatures from 1573 to 1673 K showed that samples of hot-pressed silicon nitride displayed higher creep strains and lower creep strengths than those for the reaction-bonded materials tested. However, a sialon sample (with $z = 1$) was found to exhibit creep properties which were comparable with those for the RBSN testpieces studied, indicating that sialons can be prepared having creep strengths at least equal to those for reaction-bonded products.

(2) Several fabrication variables were found to influence the creep properties of reaction-bonded silicon nitride. In particular, the creep strength was decreased significantly by the presence of small quantities (in the range 0.06 to 0.3%) of refractory oxides, with CaO having the most pronounced effect. When the creep resistance was defined in terms of the creep strains recorded in a specified time, the creep strains observed for RBSN samples appeared to be decreased by achieving larger weight gains during nitriding and by increasing the average size of the initial silicon powder. In contrast, improving the purity of the silicon powder beyond normal commercial levels did not seem to affect the creep properties.

(3) Although the creep strength of silicon carbide was found to be markedly greater than that for the hot-pressed silicon nitride samples tested, the incorporation of silicon carbide particles into samples of HPSN did not result in improved creep properties. Indeed SiC particles above a threshold size resulted in slightly increased creep rates and significantly decreased creep ductilities, with the threshold size decreasing with larger volume fractions of silicon carbide. Moreover, with SiC particles above the threshold size, the non-equiaxed nature of the particles resulted in creep strengths which were dependent on whether the specimens were tested with the compression axis parallel to or perpendicular to the pressing direction.

(4) The stress and temperature dependence of the creep rate could be described by the equation

$$\dot{\epsilon}_s = A\sigma^n \exp(-Q_c/RT)$$

with $n \simeq 2.1$ to 2.4 for all materials tested. The activation energy for creep (Q_c) was $\sim 650\,\mathrm{kJ\,mol^{-1}}$ for the reaction-bonded and hot-pressed silicon nitride materials, whereas the silicon carbide and the sialon samples gave Q_c values of 730 and 850 $\mathrm{kJ\,mol^{-1}}$ respectively.

(5) For the entire range of materials studied, the creep rate appeared to be determined predominantly by the rate at which the development of grain boundary microcracks allowed relative movement of the crystals to take place.

Acknowledgement

The authors wish to acknowledge the support of the Ministry of Defence (Procurement Executive), which included a Senior Research Assistantship for Dr J. M. Birch.

References

1. A. F. McLEAN, *Bull. Amer. Ceram. Soc.* **22** (1973) 433.
2. J. S. O'NEILL, *Proc. Brit. Ceram. Soc.* **22** (1973) 355.
3. D. E. HARRISON, *ibid.* (1973) 391.
4. K. H. JACK, *J. Mater. Sci.* **11** (1976) 1135.
5. N. L. PARR, G. F. MARTIN and E. R. W. MAY. "Special Ceramics", Vol. 1 (British Ceramic Research Association, Stoke-on-Trent, 1960) p. 102.
6. E. GLENNY and T. A. TAYLOR, *Powder Met.* 8 (1961) 164.
7. W. ENGEL and F. THUMMLER, *Ber. Dt. Keram. Ges.* **50** (1973) 204.
8. W. ASHCROFT, *Proc. Brit. Ceram. Soc.* **22** (1973) 169.
9. J. A. MANGELS, "Ceramics for High Performance Applications", edited by J. J. Burke, A. E. Gorum and R. B. Karz (Brook–Hill, Mass., 1974) p. 195.
10. S. U. DIN and P. S. NICHOLSON, *J. Amer. Ceram. Soc.* **58** (1975) 500.
11. *Idem, J. Mater. Sci.* **10** (1975) 1375.
12. N. J. OSBORNE, *Proc. Brit. Ceram. Soc.* **25** (1975) 263.

13. R. KOSSOWSKY, D. J. MILLER and E. S. DIAZ, *J. Mater. Sci.* **10** (1975) 983.
14. J. M. BIRCH and B. WILSHIRE, *ibid.* 9 (1974) 794.
15. D. J. GODFREY and M. W. LINDLEY, *Proc. Brit. Ceram. Soc.* **22** (1973) 229.
16. R. F. COE, R. J. LUMBY and M. F. PAWSON, "Special Ceramics", Vol. 5 (British Ceramic Research Association, Stoke-on-Trent, 1972) p. 361.
17. J. M. BIRCH, B. WILSHIRE, D. J. R. OWEN and D. SHANTARAM, *J. Mater. Sci.* **11** (1976) 1817.
18. J. M. BIRCH, B. WILSHIRE and D. J. GODFREY, *Proc. Brit. Ceram. Soc.* **26** (1978) 141.
19. R. KOSSOWSKY, "Ceramics for High Performance Applications", edited by J. J. Burke, A. E. Gorum and R. B. Katz (Brook-Hill, Mass., 1974) p. 347.
20. J. L. ISHOE, E. F. LANGE and E. S. DIAZ, *J. Mater. Sci.* **11** (1976) 908.
21. D. S. THOMPSON and P. L. PRATT, *Proc. Brit. Ceram. Soc.* **6** (1966) 37.
22. M. H. LEWIS, B. D. POWELL, P. DREW, R. J. LUMBY, B. NORTH and A. J. TAYLOR, *J. Mater. Sci.* **12** (1977) 61.
23. J. E. RESTALL and G. R. GESTELOW, *Proc. Brit. Ceram. Soc.* **22** (1973) 89.
24. P. L. FARNSWORTH and R. L. COBLE, *J. Amer. Ceram. Soc.* 49 (1966) 264.
25. T. L. FRANCIS and R. L. COBLE, *ibid.* **51** (1968) 115.
26. P. MARSHALL and R. B. JONES, *Powder Met.* **12** (1969) 193.
27. A. G. EVANS and J. V. SHARP, *J. Mater. Sci.* **6** (1971) 1292
28. A. G. EVANS and T. G. LANGDON, *Prog. Mater. Sci.* **21** (1976) 171.
29. F. R. N. NABARRO, "Strength of Solids" (The Physical Society, London, 1948) p. 75.
30. C. HERRING, *J. Appl. Phys.* **21** (1950) 437.
31. R. L. COBLE, *ibid.* 34 (1963) 1679.
32. K. JAMES and K. H. G. ASHBEE, *Prog. Mater. Sci.* **21** (1975) 1.
33. R. ROSSIN, J. BERSAN and G. URBAIN, *Rev. Hautes Temp. Refract.* **1** (1964) 159.
34. F. F. LANGE, "Deformation of Ceramics", edited by R. C. Brant and R. Tressler (Plenum, New York, 1975).
35. A. G. EVANS, L. R. RUSSELL and D. W. RICHERSON, *Metall. Trans.* **6** (1975) 707.
36. D. P. H. HASSELMAN and E. P. CHEN, *J. Amer. Ceram. Soc.* **60** (1977) 76.
37. J. A. WILLIAMS, *Phil. Mag.* **20** (1969) 635.
38. A. CROSBY and P. E. EVANS, *J. Mater. Sci.* 8 (1973) 1579.
39. E. GLENNY and R. A. TAYLOR, *Powder Met.* 5 (1958) 185.
40. G. GRATHWOHL and F. THUMMLER, *Ber. Dt. Keram. Ges.* **52** (1975) 268.
41. D. J. GODFREY, *Proc. Brit. Ceram. Soc.* **25** (1975) 325.
42. *Idem, ibid.* **26** (1978) 265.
43. N. L. PARR and G. F. MARTIN "Special Ceramics", Vol. 1 (British Ceramic Research Association, Stoke-on-Trent, 1960) p. 76.
44. F. F. LANGE, *J. Amer. Ceram. Soc.* **56** (1973) 445.

Received 28 February and accepted 28 April 1978.